Published in final edited form as:

Cancer Res. 2018 May 01; 78(9): 2277–2289. doi:10.1158/0008-5472.CAN-17-2899.

A soft microenvironment protects from failure of midbody abscission and multinucleation downstream of the EMT-promoting transcription factor Snail

Allison K. Simi[1], **Alişya A. Anlaş**[1], **Melody Stallings-Mann**[3], **Sherry Zhang**[1], **Tiffaney Hsia**[1], **Magdalena Cichon**[3], **Derek C. Radisky**[3], and **Celeste M. Nelson**[1,2,*]

[1]Department of Chemical & Biological Engineering, Princeton University, Princeton, NJ 08544

[2]Department of Molecular Biology, Princeton University, Princeton, NJ 08544

[3]Department of Cancer Biology, Mayo Clinic Cancer Center, Jacksonville, FL 32224

Abstract

Multinucleation is found in more than one third of tumors and is linked to increased tolerance for mutation, resistance to chemotherapy, and invasive potential. The integrity of the genome depends on proper execution of the cell cycle, which can be altered through mechanotransduction pathways as the tumor microenvironment stiffens during tumorigenesis. Here we show that signaling downstream of matrix metalloproteinase-3 (MMP3) or transforming growth factor-β (TGFβ), known inducers of epithelial-mesenchymal transition (EMT), also promotes multinucleation in stiff microenvironments through Snail-dependent expression of the filament-forming protein septin-6, resulting in midbody persistence, abscission failure, and multinucleation. Consistently, we observed elevated expression of Snail and septin-6 as well as multinucleation in a human patient sample of metaplastic carcinoma of the breast, a rare classification characterized by deposition of collagen fibers and active EMT. In contrast, a soft microenvironment protected mammary epithelial cells from becoming multinucleated by preventing Snail-induced upregulation of septin-6. Our data suggest that tissue stiffening during tumorigenesis synergizes with oncogenic signaling to promote genomic abnormalities that drive cancer progression.

Keywords

aneuploidy; mechanosensing; mechanotransduction; substratum stiffness

Introduction

All cancers are genomically unstable and the most common type of genomic instability is chromosomal instability, or an increased rate of chromosome missegregation. Chromosomal instability is characterized by aneuploidy, which is defined as an abnormal number of chromosomes and is found in 85% of all solid cancers, including 85% of breast tumors (1).

*Address correspondence to C.M.N., 303 Hoyt Laboratory, William Street Princeton, NJ 08544, Tel: 609-258-8851, Fax: 609-258-1247, celesten@princeton.edu.

Conflict of interest statement: The authors declare no potential conflicts of interest.

Even in the absence of other defects, induction of aneuploidy is sufficient to promote tumorigenesis *in vivo* (2). Failure of mitosis that results in multinucleation can lead to aneuploidy – multinucleated cells that continue to divide will commonly produce aneuploid progeny of varying chromosomal arrangements (3), and there is mounting evidence that multinucleation is both common in cancer and indicative of tumor prognosis: an analysis of eleven types of cancer from The Cancer Genome Atlas found that 37% percent of tumors exhibit whole-genome doubling (WGD), which typically precedes other somatic copy number alterations (4). A comparison of *in situ* breast carcinomas revealed that multinucleation is more common in pleomorphic lobular carcinoma than in the less invasive classical lobular or ductal carcinomas, suggesting that multinucleation may be associated with invasive potential (5). Furthermore, induction of tetraploidy in human cells promotes increased tolerance for mutation, resistance to chemotherapeutic drugs, and transformation in culture (6).

In addition to being genomically unstable, tumors are generally stiffer than normal tissue. Enhanced deposition and crosslinking increases the density of the extracellular matrix (ECM) in tumors and stiffness is a common diagnostic parameter. Mechanosensors mediate the balance between extracellular forces and intracellular cytoskeletal tension and in doing so translate physical changes in the microenvironment to chemical signals inside the cell. Signaling triggered by stiffening of the ECM can induce changes in phenotype and gene expression that result in deleterious consequences, including cancer progression. For example, the ability of matrix metalloproteinase-3 (MMP3; stromelysin-1) to induce epithelial-mesenchymal transition (EMT) in mammary epithelial cells depends on the subcellular localization of the Rac1 splice variant Rac1b, which is modulated by the stiffness of the surrounding microenvironment. MMP3 is a secreted protease commonly upregulated in cancer that induces expression of Rac1b. Stiff substrata, with compliances characteristic of breast tumors, cause activation and clustering of integrins, which promotes localization of Rac1b to the plasma membrane, activation of NADPH oxidase, production of reactive oxygen species (ROS), and elevated expression of the key EMT effector and transcription factor, Snail. Soft substrata, with compliances characteristic of normal mammary tissue, prevent Rac1b membrane localization and protect against EMT (7).

Through their primary role in remodeling the ECM, MMPs induce many changes in the surrounding cells, EMT serving as just one example. Notably, MMPs were previously linked to genomic instability in culture and *in vivo*. MMP3 in particular was found to increase the resistance of mouse mammary epithelial cells to *N*-(phosphonacetyl)-L-aspartate (PALA) through amplification of the *CAD* locus downstream of ROS, in addition to causing other genomic amplifications and deletions similar to those observed in transgenic mice that ectopically express MMP3 in the mammary gland (8,9). Similarly, transforming growth factor-beta (TGFβ) is a potent inducer of EMT that has also been implicated in genomic instability, including promotion of multinucleation in MCF10A mammary epithelial cells (10). The ability of TGFβ to induce EMT in mammary epithelial cells is likewise regulated by substratum stiffness (11).

Although the mechanical properties of the microenvironment have previously been shown to regulate the cell cycle (12,13), and proper regulation of the cell cycle is intrinsically

connected to the stability of the genome, a link between abnormal mechanical properties in the cellular microenvironment and induction of genomic instability has not been established. We show here that matrix stiffness regulates multinucleation in mammary epithelial cells. By evaluating how cells respond to EMT inducers when cultured on engineered two-dimensional (2D) polyacrylamide substrata of varying stiffness, we found that multinucleation is increased on stiff substrata through failure of midbody abscission as a consequence of the expression of septin-6, a novel target of Snail. A soft microenvironment appears to protect the stability of the genome in epithelial cells by preventing septin-6 overexpression. Taken together, our data provide evidence that tissue stiffening during tumorigenesis synergizes with EMT-associated pathways to promote genomic abnormalities that drive cancer progression.

Materials and Methods

Cell culture and reagents

p53-mutant SCp2 mouse mammary epithelial cells that express autoactivated MMP3 under the control of the tetracycline promoter (8) were cultured in DMEM:F12 supplemented with 2% fetal bovine serum (FBS; Atlanta Biologicals), 10 μg/mL insulin, 50 μg/mL gentamicin, and 125 μg/mL geneticin (AG Scientific). To repress MMP3 expression, a 4 mg/mL stock solution of tetracycline (Sigma Aldrich) was added directly to the culture medium at a 1:800 dilution; tetracycline was removed from the medium to induce expression of MMP3. NMuMG cells (ATCC) were cultured in DMEM:F12 supplemented with 10% FBS, 10 μg/mL insulin, and 50 μg/mL gentamicin. MCF10A human mammary epithelial cells (ATCC) were cultured in DMEM:F12 supplemented with 5% horse serum (Fisher Scientific), 20 ng/ml epidermal growth factor (EGF; Sigma), 0.5 mg/mml hydrocortisone (Fisher Scientific), 100 ng/ml cholera toxin (Sigma), 10 μg/ml insulin, and 5 mg/ml gentamicin. All cell lines were authenticated by short tandem repeat genotyping (ATCC), tested for mycoplasma contamination (Lonza), and used before passage 35 (SCp2 cells), 20 (NMuMG cells), or 25 (MCF10A cells). The following reagents were added directly to fresh culture medium 24 hr after plating cells: H_2O_2, 25 μM; N-acetyl-cysteine (NAC, Sigma Aldrich), 10 mM; recombinant TGFβ1 (R&D Systems), 10 ng/mL. Cells were exposed to H_2O_2 or NAC for 72 hr and to TGFβ for 48 hr. To increase proliferation of SCp2 cells on soft substrata, 100 ng/ml of EGF was added to the culture medium for 48 hr.

Synthetic substrata

Polyacrylamide (PA) substrata were generated as described previously (7,14). Briefly, PA gels were polymerized directly on 31-mm-diameter glass coverslips as follows: 12.5% (vol/vol) acrylamide was mixed with bis-acrylamide in water at either 0.5% (vol/vol) or 17.5% (vol/vol). Polymerization was initiated by adding 10% ammonium persulfate (BioRad) at a 1:200 dilution and N,N,N',N'-tetramethylethylenediamine (Sigma Aldrich) at a 1:2000 dilution. 36 μL of the mixture was sandwiched between coverslips for 40 min at room temperature. PA gels were stored in PBS at 4°C and characterized as previously described (7).

The surfaces of the PA gels were then functionalized with 200 μg/ml fibronectin (BD Biosciences) as described previously using the heterobifunctional crosslinker Sulfo-SANPAH (Thermo Scientific) (14). Before plating cells, gels were washed three times with PBS and incubated with culture medium for 30 min at 37°C. To achieve a final density of ~15,000 cells/cm^2, we initially seeded 8×10^5, 4×10^5, or 1.5×10^5 cells onto soft, stiff, or bare coverslips in wells of a 6-well plate.

Transfections and viral transductions

SCp2 cells were transfected or transduced in medium containing tetracycline, with the exception of the MMP3 +/− NAC and MMP3 +/− shSnail experiments, which were performed under tetracycline withdrawal. pMK782 Septin6-GFP was obtained from AddGene (plasmid # 38296). pEYFP-C1 was obtained from BD Biosciences (catalog #6005-1). Plasmids were transfected using FuGENE HD Transfection Reagent (Promega). Briefly, FuGENE and DNA were mixed in Opti-MEM medium (2:1 ratio for SCp2 cells; 3:1 for NMuMG cells) and added directly to culture medium, which was changed 20 hr later. Cells were fixed and analyzed 24 hr later.

Recombinant adenoviruses encoding YFP-Rac1b, YFP-Rac1b-SAAX, YFP-Rac1b-myr, Aurora A kinase, shRNA against Snail (shSnail) or GFP were obtained from Vector BioLabs (7). Recombinant adenovirus encoding GFP-Snail was a gift from Paul Wade (National Institute of Environmental Health Sciences, Research Triangle Park, NC). Adenovirus was added directly to culture medium at an MOI of 100, and medium was changed 24 hr after transduction. Cells were fixed and analyzed 24 hr later.

Reverse transcriptase quantitative polymerase chain reaction (RT-qPCR)

Gene expression was assessed by RT-qPCR 72 hr after inducing expression of MMP3 or 48 hr after exposing cells to all other conditions. RNA was extracted using TRIzol reagent (Invitrogen), followed by cDNA synthesis using a Verso cDNA synthesis kit (Thermo Scientific). Transcript levels were measured using an Applied Biosystems Step One Plus instrument and iTaq Supermix with SYBR green chemistry. Amplification was followed by melt-curve analysis to verify the presence of a single PCR product. Primers (Table S1) were designed using PrimerQuest (Integrated DNA Technologies) and determined to be specific by BLAST. The expression level of each mRNA was normalized to that of 18S in the same sample.

Immunofluorescence staining

Samples were fixed with 4% paraformaldehyde in PBS for 20 min at room temperature, followed by three washes with PBS. To label E-cadherin, MKLP1, or Ki67, samples were blocked with 10% (vol/vol) goat serum (Sigma Aldrich) in PBS for 4 hr, and incubated overnight at 4°C with rabbit anti-E-cadherin antibody (Cell Signaling), rabbit anti-MKLP1 antibody (Abcam), or mouse anti-Ki67 antibody (Cell Signaling), respectively. Samples were washed 6 times with 0.3% Triton-X-100 in PBS (PBST) for 30 min each time, and incubated with Alexa 594 goat anti-rabbit secondary antibody (Invitrogen) overnight at 4°C. To label nuclei, samples were incubated with a 1:1000 dilution of Hoechst 33342

(Invitrogen) for 20 min at room temperature and washed 3 times with PBS for 10 min each time.

To label centrosomes, samples were fixed with 100% methanol for 20 min at −20°C, followed by three washes with PBS. Samples were blocked as described above and incubated with rabbit anti-γ-tubulin (Santa Cruz Biotechnology) overnight at 4°C. Samples were washed and incubated with secondary antibody as described above.

To assess proliferation rate in response to treatment with EGF, samples were incubated with 10 μM EdU for one hour before fixation, permeabilization, and EdU staining, using the Click-iT EdU Alexa Fluor 594 Imaging kit (Thermo Scientific) according to the manufacturer's instructions.

Metaphase spreads

Metaphase spreads were prepared following a standard protocol using colcemid and KCl. Briefly, cells were treated with 0.5 μg/mL colcemid for 18–20 hr. Cells in metaphase were collected by treatment with trypsin for 5 min, followed by centrifugation in culture medium for 5 min at 2500 rpm. Pellets were resuspended by adding 0.075 M KCl dropwise and then incubated at 37°C for 20 min. Cells were centrifuged for 5 min at 2500 rpm, resuspended in methanol:acetic acid (3:1), and incubated on ice for 20 min. To wash, cells were centrifuged and resuspended in fixative 3 more times. The third time, cells were resuspended in 250 μL of fixative, and 20 μL of the suspension was dropped on the center of a microscope slide held at a 45° angle. Drops were dried in a pre-humidified chamber for 15 min at 37°C. Spreads were mounted using Fluoromount-G with DAPI (Southern Biotech) and sealed with clear nail polish before imaging.

Immunoblotting analysis

Samples were lysed in RIPA lysis buffer (Thermo Scientific) supplemented with protease inhibitors (Roche) and protein concentrations were measured using the Pierce bicinchoninic acid (BCA) Protein Assay Kit (Thermo Scientific). Samples were then mixed with Laemmli sample buffer, boiled at 95°C for 5 min, resolved by SDS-PAGE, and transferred to nitrocellulose membranes. Membranes were then blocked in 5% milk and incubated overnight at 4°C in blocking buffer containing antibodies specific for septin-6 (Lifespan Biosciences) or GAPDH (Cell Signaling).

Imaging and quantification

Still images were acquired using a Hamamatsu Orca CCD camera attached to a Nikon Ti-U inverted fluorescence microscope at 20× magnification in air (or 60× magnification in oil for metaphase spreads). Phase contrast and fluorescence images were merged using ImageJ. For multinucleation experiments, cells with two or more nuclei were counted and recorded as the percentage of the total number of cells in each image. The number of images needed to accurately quantify an experimental condition was determined using a running average. Briefly, the total percentage of multinucleated cells was adjusted as each additional image was analyzed. When the percentage of multinucleation stabilized, no further images were analyzed. Similar methodology was used to quantify centrosome amplification and

multipolar mitosis. For metaphase spreads, total chromosomes per cell were counted for 30–36 cells. Aneuploidy was defined as the number of chromosomes per cell normalized to the average number of chromosomes per cell in a population.

Timelapse movies were acquired using a Hamamatsu C4742-95 camera attached to a Nikon Ti-U inverted microscope and fitted with an environmental chamber held at 90% humidity, 37°C, and 5% CO_2. Images were acquired at 10× magnification every 3 min for a total of 8 hr, and stacked in ImageJ.

Histological analysis of tissue samples

Breast cancer biopsies were derived from waste surgical material from de-identified patients, and were formalin-fixed and paraffin-embedded, as per approval by the Mayo Clinic Institutional Review Board. Tissue sections (4 or 10 μm) were deparaffinized by placing them into three changes of xylene and rehydrated in a graded ethanol series. The rehydrated tissue samples were rinsed in water and sections were subjected to heat antigen retrieval as described by the manufacturer (DAKO) using citrate buffer pH 6.0. Slices were incubated with each primary antibody for 1 hr at room temperature. Sections were then rinsed with Tris-buffered saline/Triton-X-100 (TBST) wash buffer, and incubated with each secondary antibody for 30 min. For fluorescent detection, tissue sections were rinsed 3 times for 5 min each with PBS containing 1.43 μM 4′,6-diamidino-2-phenylindole (DAPI; Thermo Fisher Scientific). Sections were incubated with primary antibody (Snail or septin-6), rinsed with TBST wash buffer, and incubated with secondary antibody (DAKO Envision anti-rabbit, HRP for 30 min (Snail) or anti-goat HRP (Biocare) for 30 min (septin-6)). Tissue sections were rinsed with TBST wash buffer and then incubated in 3,3′-diaminobenzidine (DAB+; DAKO), and counterstained with Gills I hematoxylin. Each antibody and its corresponding fluorescent secondary antibody used were: Snail (rabbit polyclonal, Bioworld Technology #BS1853) detected by Alexa488-conjugated donkey anti-rabbit IgG (Invitrogen, #A21202); septin-6 (goat polyclonal, Lifespan #LS-B9200) detected by Alexa594-conjugated donkey anti-goat IgG (H+L) (Invitrogen, A11058).

Whole slide digital images of each breast cancer sample were captured with the Aperio Scanscope AT2 slide scanner (H&E, Snail, septin-6) and the Aperio Scanscope FL slide scanner (fluorescent images) using a 20× objective. For quantification of multinucleated cells, serial sections of breast cancer biopsy samples were stained with H&E and Snail. The IHC-stained images were used as guides to demarcate areas digitally of high and low Snail expression in a thick (10 μm) H&E stained section. The regions were of equal size (153680.90 um^2) and were spread among the areas of low (n=10) or high (n=10) Snail expression. Multinucleated cells were identified and counted in each selected area.

Statistical analysis

Data represent mean ± SEM of at least three independent experiments. Statistical analysis was conducted using a Student t-test or a one- or two-way ANOVA followed by Bonferroni post-tests. For the patient samples, data represent mean ± SEM of 10 regions of stained sections, and statistical significance was tested with the Mann-Whitney test. $p < 0.05$ was considered to represent a significant difference between conditions.

Results

MMP3 promotes genomic instability by causing multinucleation

In addition to inducing EMT in mammary epithelial cells, MMP3 has been found to induce genomic instability. We characterized MMP3-induced genomic instability using a derivative of SCp2 cells with a tet-inducible auto-activated MMP3 (8). These cells lack functional p53, which is required for survival of multinucleated cells (15). Consistently, metaphase spreads revealed that exposure to MMP3 induced aneuploidy (Figure 1A,B). Aneuploid progeny often result from cells with an elevated number of centrosomes, a phenotype commonly associated with multinucleation. Amplified centrosomes can cause multipolar mitoses or cluster at opposite poles and give rise to merotelic attachments and lagging chromosomes (16). We sought to determine whether the chromosomal aberrations observed in MMP3-treated cells were downstream of multinucleated intermediates.

Staining for γ-tubulin and DNA revealed that treatment with MMP3 resulted in centrosome amplification (Figure 1C,D) and multipolar and clustered mitoses (Figure 1E,F). Similarly, staining for E-cadherin and DNA revealed a higher fraction of multinucleation in cells expressing MMP3 (Figure 1G,H). MMP3-induced genomic instability was previously found to occur downstream of ROS (8). Consistently, we found that MMP3-induced centrosome amplification and multinucleation were ameliorated by treatment with the ROS scavenger N-acetyl-cysteine (NAC) (Figure 1D, 1H). These data suggest that MMP3-associated genomic instability arises, in part, as a consequence of multinucleation.

MMP3-induced multinucleation is regulated by substratum stiffness

We previously found that EMT-associated signaling downstream of MMP3 is regulated by the mechanical stiffness of the microenvironment (7). To determine whether MMP3-induced multinucleation is similarly regulated by matrix stiffness, we cultured cells on polyacrylamide gels of various stiffness in the presence or absence of MMP3 (Figure 2A). Substrata with Young's moduli of 130 Pa and 4020 Pa mimicked the mechanical properties of physiologically normal breast tissue and tumor tissue, respectively, and are hereafter referred to as "soft" and "stiff" (7). We found that treatment with MMP3 induced multinucleation on stiff but not soft substrata (Figure 2B).

MMP3 induces the expression of the Rac1 splice variant Rac1b, which on stiff substrata localizes to the plasma membrane and associates with NADPH oxidase to produce ROS, thus leading to upregulation of Snail (7). To determine if this MMP3-induced signaling pathway regulates multinucleation (Figure 2C), we paired overexpression and knockdown experiments for Rac1b, ROS, and Snail. Ectopic expression of Rac1b induced multinucleation on stiff substrata independently of exposure to MMP3 (Figure 2D,E). Forcing Rac1b to localize to the membrane by expressing a mutant that contains an additional membrane-targeting myristoylation sequence (Rac1b-myr) further increased multinucleation on stiff substrata. In contrast, preventing Rac1b membrane localization by expressing a mutant that blocks prenylation (Rac1b-SAAX) reduced multinucleation on stiff substrata (Figure 2D,F). Similarly, increasing ROS in the absence of MMP3 by treating cells with H_2O_2 promoted multinucleation on stiff substrata (Figure 2G), whereas quenching ROS

by treating with NAC decreased the ability of MMP3 to induce multinucleation on stiff substrata (Figure 2H). Finally, ectopic expression of Snail induced multinucleation on stiff substrata independently of exposure to MMP3 (Figure 2I) or cell doubling time (Figure S1A,B). Depleting Snail by using short hairpin RNA (shRNA) decreased MMP3-induced multinucleation on stiff substrata (Figure 2J). These data suggest that on stiff substrata, MMP3 induces multinucleation by signaling through Rac1b, ROS, and Snail. Importantly, a soft microenvironment appears to protect cells from becoming multinucleated in response to this pathway. Cells on soft substrata were impervious to becoming multinucleated even when their proliferation rate was elevated by treatment with exogenous growth factor (Figure S1C,D).

Snail induces multinucleation by increasing midbody persistence

Ectopic expression of Snail did not induce multinucleation on soft substrata (Figure 2I). Thus, we reasoned that in addition to influencing the localization of Rac1b, substratum stiffness must modulate signaling downstream of Snail. We therefore sought to understand the mechanism by which Snail could promote multinucleation.

Oncogenic induction of multinucleation has been found to occur through at least two physical mechanisms. Timelapse imaging of malignant cells in culture has suggested that multinucleation results from a failure of cytokinesis (17). Cancerous mutations in *BRCA2* are linked to multinucleation by causing a failure of cytokinesis upon improper regulation of the midbody (18). Conversely, it is well recognized that cell-cell fusion can promote tumor progression. For example, oncogenic fusion can result from dysregulated expression of fusogenic proteins such as CD44 (19) or syncytin (20). We investigated both physical mechanisms in the context of Snail signaling.

Previous microarray data revealed that Aurora A kinase (AURKA) is upregulated in mammary epithelial cells in response to MMP3 exposure (21). Overexpression of AURKA is common in several cancers and linked to multinucleation by causing a failure of cytokinesis (22). In contrast to previous studies, we found that ectopic expression of AURKA did not induce multinucleation in cells cultured on soft or stiff substrata (Figure S2A). Similarly, neither fusogenic protein CD44 nor syncytin was identified as a new target of Snail that would lead to multinucleation (Figure S2B,C).

Since Snail did not appear to induce multinucleation through cell-cell fusion, we turned to timelapse microscopy to visualize the cell division process in response to ectopic expression of Snail. Phase contrast images suggested that multinucleation in cells overexpressing Snail was frequently preceded by a persistent midbody, which appeared as a phase-dense structure between two daughter cells (Figure 3A, Movies S1, 2). Midbodies are organelles created by compaction of the mid-zone of the mitotic spindle, a dense collection of overlapping microtubules that serves to spatially orient the cleavage furrow during cytokinesis (23). The final stage of cytokinesis is midbody abscission, a complex orchestration involving hundreds of proteins during which the cytokinetic bridge is severed on one or both sides of the midbody. The resulting structure, referred to as the midbody descendent (MB^D), is either pulled by its tether into the cytoplasm of the attached daughter cell or released into the intercellular space and subsequently engulfed and degraded by one of the daughter cells

(24,25). Midbody persistence can result in abscission failure and multinucleation, and is evidenced here by accumulation of MB^Ds.

To determine if signaling downstream of Snail causes multinucleation by increasing midbody persistence, we quantified MB^Ds in cells that ectopically expressed Snail. MB^Ds were identified as puncta in cells stained for the midbody marker mitotic kinesin-like protein (MKLP1) (Figure 3B). Quantification of MKLP1-positive puncta revealed that a significantly higher fraction of multinucleated cells had MB^Ds than did mononucleated cells (Figure 3C). MB^Ds were previously found to accumulate in cancer cells, which contributes to tumorigenicity in culture (26). We hypothesized that as multinucleated cells continued to divide, persistent midbodies would accumulate. Accordingly, we found that a significantly higher fraction of multinucleated cells than mononucleated cells had accumulated at least two MB^Ds. This difference was exacerbated in cells ectopically expressing Snail (Figure 3D). Together, these data suggest that Snail increases midbody persistence, which prevents or delays abscission and results in multinucleation.

MKLP1 is a kinesin-like protein that is necessary for cytokinesis (27) and stabilizes the interaction between the midbody and the cortex (28). We therefore asked whether dysregulation of MKLP1 or other kinesins caused errors in abscission or induced multinucleation downstream of Snail. We found that ectopically expressing Snail did not change the levels of MKLP1 (Figure S2D) or other kinesin family members (Figure S2E), suggesting that these proteins are not responsible for Snail-induced multinucleation.

Snail and substratum stiffness elevate septin-6 to increase midbody persistence

How does Snail enhance midbody persistence and accumulation, and subsequently, multinucleation? Previous microarray data showed that centromere-associated protein E (CENP-E), which localizes to the midbody and is degraded before abscission (29), is upregulated in response to MMP3 (21). Similarly, degradation of Aurora B kinase (AURKB) at the midbody is necessary for complete abscission, and its dysregulation results in tetraploidy (30). However, neither CENP-E nor AURKB levels were affected by ectopic expression of Snail (Figure S2F,G).

We therefore examined the role of septins, a family of filament-forming GTPases. The actomyosin contractile ring is anchored to the midbody by septin-anillin complexes, which also aid the recruitment of abscission machinery to the midbody (31). In doing so, and in direct interactions with microtubule-binding proteins such as MAP4 (32), septins facilitate microtubule depolymerization and the completion of cytokinesis. Dysregulation of septins can result in multinucleation, developmental errors, and embryonic lethality (33–35).

We assessed the levels of septins in Snail-expressing cells and found that Snail caused an increase in the core-filament-forming septin-6 (Figure 4A), but not the other core septins-2 or -7 (Figure S2H,I). Similarly, we found no change in the level of septin-9, previously associated with errors in midbody abscission and multinucleation (33), or septin-4, previously found to be downregulated in response to MMP3 (21) (Figure S2J,K). Consistently, expression of a septin6-GFP fusion protein induced midbody persistence (Figure 4B), MB^D accumulation (Figure 4C,D), and multinucleation (Figure 4E) in the

absence of ectopic Snail. We also found that septin6-GFP colocalized with the developing midbody as cells progressed through mitosis (Figure 4F). These data suggest that septin-6 is specifically involved in Snail-induced multinucleation.

To test the hypothesis that substratum stiffness modulates signaling downstream of Snail, we asked whether stiffness affects the expression of septin-6 and induction of midbody persistence. As predicted, we found higher levels of septin-6 transcript (Figure 4G) and protein (Figure 4H) in cells cultured on stiff substrata than in those on soft substrata. Additionally, quantification of MKLP1-positive puncta showed that a higher fraction of cells cultured on stiff substrata had MB^Ds than cells cultured on soft substrata (Figure 4I).

Stiffness regulates multinucleation through EMT signaling pathways

Because MMP3 leads to both EMT and multinucleation in a stiffness-dependent manner, we hypothesized that multinucleation might be a general response to EMT inducers, which commonly elevate the expression of Snail. To test this hypothesis, we treated cells with the EMT-inducer TGFβ (Figure 5A) and quantified subsequent levels of multinucleation. Similar to signaling downstream of MMP3, treatment with TGFβ enhanced the expression of Snail (Figure 5B) and septin-6 (Figure 5C). Furthermore, treatment with TGFβ resulted in significantly more multinucleated cells (Figure 5D) than controls, and staining for MKLP1 revealed that a significantly higher fraction of multinucleated cells had MB^Ds than did mononucleated cells (Figure 5E). As with MMP3, TGFβ-induced multinucleation was inhibited on soft substrata (Figure 5F). Similarly, we found that treating NMuMG mouse mammary epithelial cells with TGFβ significantly enhanced the expression of Snail (Figure 5G) and septin-6 (Figure 5H) and increased multinucleation (Figure 5I) only on stiff substrata. Altogether, our data suggest that the increased levels of Snail observed during the EMT program drive multinucleation on stiff substrata by upregulating septin-6, which increases midbody persistence and leads to abscission failure.

We also found that expression of Snail induced multinucleation in MCF10A human mammary epithelial cells (Figure S3A), a spontaneously immortalized line derived from fibrocystic breast tissue that is generally considered normal because the cells are not malignant (36). Consistent with our observations of the mouse mammary epithelial cell lines, we found that Snail only induced multinucleation of MCF10A cells when they were cultured on stiff substrata (Figure S3A) and that the multinucleated cells were associated with an increase in MB^Ds (Figure S3B). Curiously, culture on stiff substrata elevated the expression of septin-6 as well as septin-2 and -7 (Figure S3C), suggesting the possibility of a tighter co-regulation of the core septins in these cells.

Multinucleation is elevated in regions of high Snail expression in metaplastic carcinoma

To evaluate the relationship between EMT signaling, abscission failure, and multinucleation *in vivo*, we examined the expression of Snail and septin-6 and quantified multinucleation in human breast cancer samples. Histological analysis revealed Snail and septin-6 double-positive tumor cells in a metaplastic carcinoma sample, a rare cancer characterized by the presence of both epithelial- and mesenchymal-like cells, in which EMT is believed to be active (37,38) (Figure 6A; Figure S4A). In regions containing high levels of Snail, nearly

4% of cells were multinucleated, compared to less than 1% of cells in regions with low levels of Snail (Figure 6B,C). Relative collagen content is highly correlated with stiffness in mammary cancers (39,40), and we found high expression of Snail and septin-6 specifically in tumor regions with high collagen (Figure 6D–E). Consistently, the level of septin-6 expression correlates with degree of multinucleation (Figure S4B). These data are consistent with our experiments in culture, and suggest that EMT signaling, through Snail and septin-6, promotes multinucleation in stiff microenvironments.

Discussion

Mechanical signaling is known to regulate the cell cycle. For example, the orientation of the mitotic spindle is dictated by retraction fibers and the subcortical actin network in HeLa cells (12). Similarly, the spatial distribution of ECM proteins can determine the axis of division by regulating actin dynamics (13). Disruption of the cell cycle can result in cancer, but little is known about how tissue mechanics affects stability of the genome. Here, we uncovered a mechanotransduction pathway that links the mechanical properties of the microenvironment with EMT and genomic instability. Exposure to either MMP3 or TGFβ leads to increased expression of Snail, but has divergent effects on other EMT-associated transcription factors (Figure S5A,B). Snail elevates the levels of septin-6 in cells on stiff microenvironments that are characteristic of breast tumors. Septin-6 overexpression increases midbody persistence, causing a failure of midbody abscission and subsequent multinucleation (Figure 7A).

Septin filaments help anchor the actomyosin contractile ring to the plasma membrane (31). Maintaining homeostatic levels of septins-2, -6, and -7, the core filament-forming septins, is necessary to avoid mitotic errors, aneuploidy, and multinucleation (33–35). The behavior of the core septins seems closely linked; specifically depleting one can cause loss of the others (32,33,35). Thus, although septin variants can perform unique roles (33,41), concomitant loss makes this difficult to determine for the core septins. Frequent mutations and dysregulation of septins in cancer (42) necessitates continued investigation of the individual functions of the variants. It was recently determined that septins-2 and -7 contribute to both tumor suppression (43) and increased proliferation and invasion of cancer cells (44). Unique functions of septin-6 have mainly been studied in developmental contexts (45). We found that septin-6 is independently upregulated by Snail, and further, that excess septin-6, which localizes to the midbody, contributes to an increased midbody persistence, resulting in abscission failure and the eventual coalescence of the two daughter cells. These data lead us to predict that elevated levels of septin-6 downstream of Snail disrupt the balance of core septins necessary for the filament to function correctly (Figure 7B). The specific role of septin-6 in contributing to abscission failure will be the subject of a future study.

Given that Snail most commonly behaves as a transcriptional repressor, we wondered how it might induce the expression of septin-6. We found a putative Snail-binding site (CAGGTG (46)) within 1 kb upstream of the predicted transcription start sites of septin-6 in mouse and human (Table S2). Recent studies have demonstrated that Snail can act as a transcriptional activator by interacting with Twist (47) or CREB-binding protein (48). Additionally, stiff matrices enhance Twist translocation to the nucleus (49) and the expression of CREB-

binding protein (Figure S5C). With these considerations in mind, it is tempting to speculate that on stiff substrata, Snail cooperates with another factor to drive the expression of septin-6.

Our study adds to recent compelling evidence that TGFβ can induce genomic instability by disrupting cell division (10). Traditionally, TGFβ has been considered to be a suppressor of genomic instability (50) through its signaling via SMADs to activate the DNA damage response (DDR). Nonetheless, TGFβ signaling is elevated in many malignancies and correlates with enhanced metastasis (51). Since treatment with TGFβ does not alter the expression of MMP3 in our system (Figure S5D), multinucleation appears to be specific to its induction of Snail. It is likely that the mechanical properties of the microenvironment play a role in orchestrating the final outcome of exposure to TGFβ, either SMAD-mediated induction of DDR machinery or Snail-mediated induction of midbody persistence.

Metaplastic carcinoma of the breast, a rare subtype of cancer that accounts for less than 1% of breast cancer cases, is characterized by biphasic lesions containing both epithelial and mesenchymal-derived cells. These tumors are identified as rapidly growing lesions of high mammographic density (52), often contain regions of spindle-shaped, vimentin-positive cells, indicative of active EMT, and express increased reactive ECM molecules and mediators of EMT (53). In addition, metaplastic carcinomas of the breast often harbor multinucleated cells (54,55) and mutations in p53 (56). While this tumor type is relatively rare, our findings of a link between Snail, septin-6, and multinucleation may be reflective of pro-tumorigenic processes that occur in more limited regions of a broader range of breast cancers. Moreover, because tumors are stiffer than normal tissue, our findings suggest that therapies aiming to return tumor tissue to physiologically normal stiffness may prevent multinucleation and aneuploidy characteristic of genomic instability. This theory has been implicated in the clinic; chemopreventative treatment with tamoxifen has been found to lead to a reduction in mammographic density (57), which correlates with ECM density and tissue stiffness (58). Our findings suggest that cancer prevention strategies, which seek to block the earliest steps of malignant transformation, would be more effective if optimized to target the contextual cues that drive multinucleation and resultant aneuploidy.

Supplementary Material

Refer to Web version on PubMed Central for supplementary material.

Acknowledgments

This work was supported in part by grants from the NIH (GM083997, HL110335, HL118532, HL120142, and CA187692), the NSF (CMMI-1435853), the David & Lucile Packard Foundation, the Alfred P. Sloan Foundation, the Camille & Henry Dreyfus Foundation, and the Burroughs Wellcome Fund. A.K.S. was supported in part by a pre-doctoral fellowship from the New Jersey Commission on Cancer Research. C.M.N. was supported in part by a Faculty Scholar Award from the HHMI.

Abbreviations

2D	two-dimensional
3D	three-dimensional

AURKA	Aurora A kinase
AURKB	Aurora B kinase
BBD	benign breast disease
CENP	centromere-associated protein
ECM	extracellular matrix
EMT	epithelial-mesenchymal transition
MB^{D}	midbody descendant
MKLP	mitotic kinesin-like protein
MMP	matrix metalloproteinase
MNC	multinucleation
NAC	N-acetyl cysteine
PA	polyacrylamide
PALA	*N*-(phosphonacetyl)-L-aspartate
ROS	reactive oxygen species
shRNA	short hairpin RNA
SKY	spectral karyotyping
TGFβ	transforming growth factor-β
WGD	whole-genome doubling

References

1. Weaver BA, Cleveland DW. Does aneuploidy cause cancer? Curr Opin Cell Biol. 2006; 18(6):658–67. [PubMed: 17046232]
2. Weaver BA, Cleveland DW. Aneuploidy: instigator and inhibitor of tumorigenesis. Cancer Res. 2007; 67(21):10103–5. [PubMed: 17974949]
3. Ganem NJ, Storchova Z, Pellman D. Tetraploidy, aneuploidy and cancer. Curr Opin Genet Dev. 2007; 17(2):157–62. [PubMed: 17324569]
4. Zack TI, Schumacher SE, Carter SL, Cherniack AD, Saksena G, Tabak B, et al. Pan-cancer patterns of somatic copy number alteration. Nat Genet. 2013; 45(10):1134–40. [PubMed: 24071852]
5. Blanco LZ, Thurow TA, Mahajan A, Susnik B, Helenowski I, Chmiel JS, et al. Multinucleation is an objective feature useful in the diagnosis of pleomorphic lobular carcinoma in situ. Am J Clin Pathol. 2015; 144(5):722–6. [PubMed: 26486735]
6. Kuznetsova AY, Seget K, Moeller GK, de Pagter MS, de Roos JA, Durrbaum M, et al. Chromosomal instability, tolerance of mitotic errors and multidrug resistance are promoted by tetraploidization in human cells. Cell Cycle. 2015:0.
7. Lee K, Chen QK, Lui C, Cichon MA, Radisky DC, Nelson CM. Matrix compliance regulates Rac1b localization, NADPH oxidase assembly, and epithelial-mesenchymal transition. Mol Biol Cell. 2012; 23(20):4097–108. [PubMed: 22918955]

8. Radisky DC, Levy DD, Littlepage LE, Liu H, Nelson CM, Fata JE, et al. Rac1b and reactive oxygen species mediate MMP-3-induced EMT and genomic instability. Nature. 2005; 436(7047):123–7. [PubMed: 16001073]
9. Sternlicht MD, Lochter A, Sympson CJ, Huey B, Rougier JP, Gray JW, et al. The stromal proteinase MMP3/stromelysin-1 promotes mammary carcinogenesis. Cell. 1999; 98(2):137–46. [PubMed: 10428026]
10. Comaills V, Kabeche L, Morris R, Buisson R, Yu M, Madden MW, et al. Genomic Instability Is Induced by Persistent Proliferation of Cells Undergoing Epithelial-to-Mesenchymal Transition. Cell Rep. 2016; 17(10):2632–47. [PubMed: 27926867]
11. Leight JL, Wozniak MA, Chen S, Lynch ML, Chen CS. Matrix rigidity regulates a switch between TGF-beta1-induced apoptosis and epithelial-mesenchymal transition. Mol Biol Cell. 2012; 23(5): 781–91. [PubMed: 22238361]
12. Fink J, Carpi N, Betz T, Betard A, Chebah M, Azioune A, et al. External forces control mitotic spindle positioning. Nat Cell Biol. 2011; 13(7):771–8. [PubMed: 21666685]
13. Thery M, Racine V, Pepin A, Piel M, Chen Y, Sibarita JB, et al. The extracellular matrix guides the orientation of the cell division axis. Nat Cell Biol. 2005; 7(10):947–53. [PubMed: 16179950]
14. Pang MF, Siedlik MJ, Han S, Stallings-Mann M, Radisky DC, Nelson CM. Tissue Stiffness and Hypoxia Modulate the Integrin-Linked Kinase ILK to Control Breast Cancer Stem-like Cells. Cancer Res. 2016; 76(18):5277–87. [PubMed: 27503933]
15. Fujiwara T, Bandi M, Nitta M, Ivanova EV, Bronson RT, Pellman D. Cytokinesis failure generating tetraploids promotes tumorigenesis in p53-null cells. Nature. 2005; 437(7061):1043–7. [PubMed: 16222300]
16. Ganem NJ, Godinho SA, Pellman D. A mechanism linking extra centrosomes to chromosomal instability. Nature. 2009; 460(7252):278–82. [PubMed: 19506557]
17. Lv L, Zhang T, Yi Q, Huang Y, Wang Z, Hou H, et al. Tetraploid cells from cytokinesis failure induce aneuploidy and spontaneous transformation of mouse ovarian surface epithelial cells. Cell Cycle. 2012; 11(15):2864–75. [PubMed: 22801546]
18. Mondal G, Rowley M, Guidugli L, Wu J, Pankratz VS, Couch FJ. BRCA2 localization to the midbody by filamin A regulates cep55 signaling and completion of cytokinesis. Dev Cell. 2012; 23(1):137–52. [PubMed: 22771033]
19. Pawelek JM, Chakraborty AK. Fusion of tumour cells with bone marrow-derived cells: a unifying explanation for metastasis. Nat Rev Cancer. 2008; 8(5):377–86. [PubMed: 18385683]
20. Bjerregaard B, Holck S, Christensen IJ, Larsson LI. Syncytin is involved in breast cancer-endothelial cell fusions. Cell Mol Life Sci. 2006; 63(16):1906–11. [PubMed: 16871371]
21. Cichon MA, Radisky DC. ROS-induced epithelial-mesenchymal transition in mammary epithelial cells is mediated by NF-kB-dependent activation of Snail. Oncotarget. 2014; 5(9):2827–38. [PubMed: 24811539]
22. Meraldi P, Honda R, Nigg EA. Aurora-A overexpression reveals tetraploidization as a major route to centrosome amplification in p53−/− cells. EMBO J. 2002; 21(4):483–92. [PubMed: 11847097]
23. Hu CK, Coughlin M, Mitchison TJ. Midbody assembly and its regulation during cytokinesis. Mol Biol Cell. 2012; 23(6):1024–34. [PubMed: 22278743]
24. Chen CT, Ettinger AW, Huttner WB, Doxsey SJ. Resurrecting remnants: the lives of post-mitotic midbodies. Trends Cell Biol. 2013; 23(3):118–28. [PubMed: 23245592]
25. Crowell EF, Gaffuri AL, Gayraud-Morel B, Tajbakhsh S, Echard A. Engulfment of the midbody remnant after cytokinesis in mammalian cells. J Cell Sci. 2014; 127(Pt 17):3840–51. [PubMed: 25002399]
26. Kuo TC, Chen CT, Baron D, Onder TT, Loewer S, Almeida S, et al. Midbody accumulation through evasion of autophagy contributes to cellular reprogramming and tumorigenicity. Nat Cell Biol. 2011; 13(10):1214–23. [PubMed: 21909099]
27. Zhu C, Bossy-Wetzel E, Jiang W. Recruitment of MKLP1 to the spindle midzone/midbody by INCENP is essential for midbody formation and completion of cytokinesis in human cells. Biochem J. 2005; 389(Pt 2):373–81. [PubMed: 15796717]
28. Guse A, Mishima M, Glotzer M. Phosphorylation of ZEN-4/MKLP1 by aurora B regulates completion of cytokinesis. Curr Biol. 2005; 15(8):778–86. [PubMed: 15854913]

29. Liu D, Zhang N, Du J, Cai X, Zhu M, Jin C, et al. Interaction of Skp1 with CENP-E at the midbody is essential for cytokinesis. Biochem Biophys Res Commun. 2006; 345(1):394–402. [PubMed: 16682006]
30. Steigemann P, Wurzenberger C, Schmitz MH, Held M, Guizetti J, Maar S, et al. Aurora B-mediated abscission checkpoint protects against tetraploidization. Cell. 2009; 136(3):473–84. [PubMed: 19203582]
31. Menon MB, Gaestel M. Sep(t)arate or not - how some cells take septin-independent routes through cytokinesis. J Cell Sci. 2015; 128(10):1877–86. [PubMed: 25690008]
32. Kremer BE, Haystead T, Macara IG. Mammalian septins regulate microtubule stability through interaction with the microtubule-binding protein MAP4. Mol Biol Cell. 2005; 16(10):4648–59. [PubMed: 16093351]
33. Estey MP, Di Ciano-Oliveira C, Froese CD, Bejide MT, Trimble WS. Distinct roles of septins in cytokinesis: SEPT9 mediates midbody abscission. J Cell Biol. 2010; 191(4):741–9. [PubMed: 21059847]
34. Menon MB, Sawada A, Chaturvedi A, Mishra P, Schuster-Gossler K, Galla M, et al. Genetic deletion of SEPT7 reveals a cell type-specific role of septins in microtubule destabilization for the completion of cytokinesis. PLoS Genet. 2014; 10(8):e1004558. [PubMed: 25122120]
35. Spiliotis ET, Kinoshita M, Nelson WJ. A mitotic septin scaffold required for Mammalian chromosome congression and segregation. Science. 2005; 307(5716):1781–5. [PubMed: 15774761]
36. Soule HD, Maloney TM, Wolman SR, Peterson WD Jr, Brenz R, McGrath CM, et al. Isolation and characterization of a spontaneously immortalized human breast epithelial cell line, MCF-10. Cancer Res. 1990; 50(18):6075–86. [PubMed: 1975513]
37. Esses KM, Hagmaier RM, Blanchard SA, Lazarchick JJ, Riker AI. Carcinosarcoma of the breast: two case reports and review of the literature. Cases J. 2009; 2(1):15. [PubMed: 19126225]
38. Gwin K, Buell-Gutbrod R, Tretiakova M, Montag A. Epithelial-to-mesenchymal transition in metaplastic breast carcinomas with chondroid differentiation: expression of the E-cadherin repressor Snail. Appl Immunohistochem Mol Morphol. 2010; 18(6):526–31. [PubMed: 20697265]
39. Fenner J, Stacer AC, Winterroth F, Johnson TD, Luker KE, Luker GD. Macroscopic stiffness of breast tumors predicts metastasis. Sci Rep. 2014; 4:5512. [PubMed: 24981707]
40. Wang ZL, Sun L, Li Y, Li N. Relationship between elasticity and collagen fiber content in breast disease: a preliminary report. Ultrasonics. 2015; 57:44–9. [PubMed: 25465961]
41. Garcia-Fernandez M, Kissel H, Brown S, Gorenc T, Schile AJ, Rafii S, et al. Sept4/ARTS is required for stem cell apoptosis and tumor suppression. Genes Dev. 2010; 24(20):2282–93. [PubMed: 20952537]
42. Angelis D, Spiliotis ET. Septin Mutations in Human Cancers. Front Cell Dev Biol. 2016; 4:122. [PubMed: 27882315]
43. Yue X, Cao D, Lan F, Pan Q, Xia T, Yu H. MiR-301a is activated by the Wnt/beta-catenin pathway and promotes glioma cell invasion by suppressing SEPT7. Neuro Oncol. 2016; 18(9):1288–96. [PubMed: 27006177]
44. Zhang N, Liu L, Fan N, Zhang Q, Wang W, Zheng M, et al. The requirement of SEPT2 and SEPT7 for migration and invasion in human breast cancer via MEK/ERK activation. Oncotarget. 2016; 7(38):61587–600. [PubMed: 27557506]
45. Zhai G, Gu Q, He J, Lou Q, Chen X, Jin X, et al. Sept6 is required for ciliogenesis in Kupffer's vesicle, the pronephros, and the neural tube during early embryonic development. Mol Cell Biol. 2014; 34(7):1310–21. [PubMed: 24469395]
46. Nieto MA. The snail superfamily of zinc-finger transcription factors. Nat Rev Mol Cell Biol. 2002; 3(3):155–66. [PubMed: 11994736]
47. Rembold M, Ciglar L, Yanez-Cuna JO, Zinzen RP, Girardot C, Jain A, et al. A conserved role for Snail as a potentiator of active transcription. Genes Dev. 2014; 28(2):167–81. [PubMed: 24402316]
48. Hsu DS, Wang HJ, Tai SK, Chou CH, Hsieh CH, Chiu PH, et al. Acetylation of snail modulates the cytokinome of cancer cells to enhance the recruitment of macrophages. Cancer Cell. 2014; 26(4): 534–48. [PubMed: 25314079]

49. Wei SC, Fattet L, Tsai JH, Guo Y, Pai VH, Majeski HE, et al. Matrix stiffness drives epithelial-mesenchymal transition and tumour metastasis through a TWIST1-G3BP2 mechanotransduction pathway. Nat Cell Biol. 2015; 17(5):678–88. [PubMed: 25893917]
50. Barcellos-Hoff MH, Cucinotta FA. New tricks for an old fox: impact of TGFbeta on the DNA damage response and genomic stability. Sci Signal. 2014; 7(341):re5. [PubMed: 25185158]
51. Oft M, Heider KH, Beug H. TGFbeta signaling is necessary for carcinoma cell invasiveness and metastasis. Curr Biol. 1998; 8(23):1243–52. [PubMed: 9822576]
52. Luini A, Aguilar M, Gatti G, Fasani R, Botteri E, Brito JA, et al. Metaplastic carcinoma of the breast, an unusual disease with worse prognosis: the experience of the European Institute of Oncology and review of the literature. Breast Cancer Res Treat. 2007; 101(3):349–53. [PubMed: 17009109]
53. Lien HC, Hsiao YH, Lin YS, Yao YT, Juan HF, Kuo WH, et al. Molecular signatures of metaplastic carcinoma of the breast by large-scale transcriptional profiling: identification of genes potentially related to epithelial-mesenchymal transition. Oncogene. 2007; 26(57):7859–71. [PubMed: 17603561]
54. Altaf FJ, Mokhtar GA, Emam E, Bokhary RY, Mahfouz NB, Al Amoudi S, et al. Metaplastic carcinoma of the breast: an immunohistochemical study. Diagn Pathol. 2014; 9:139. [PubMed: 25030022]
55. Dwyer JB, Clark BZ. Low-grade fibromatosis-like spindle cell carcinoma of the breast. Arch Pathol Lab Med. 2015; 139(4):552–7. [PubMed: 25822766]
56. McKinnon E, Xiao P. Metaplastic carcinoma of the breast. Arch Pathol Lab Med. 2015; 139(6): 819–22. [PubMed: 26030252]
57. Cuzick J, Warwick J, Pinney E, Warren RM, Duffy SW. Tamoxifen and breast density in women at increased risk of breast cancer. Journal of the National Cancer Institute. 2004; 96:621–8. [PubMed: 15100340]
58. Schedin P, Keely PJ. Mammary gland ECM remodeling, stiffness, and mechanosignaling in normal development and tumor progression. Cold Spring Harbor perspectives in biology. 2011; 3:a003228. [PubMed: 20980442]

Significance

Findings reveal tissue stiffening during tumorigenesis synergizes with oncogenic signaling to promote genomic abnormalities that drive cancer progression

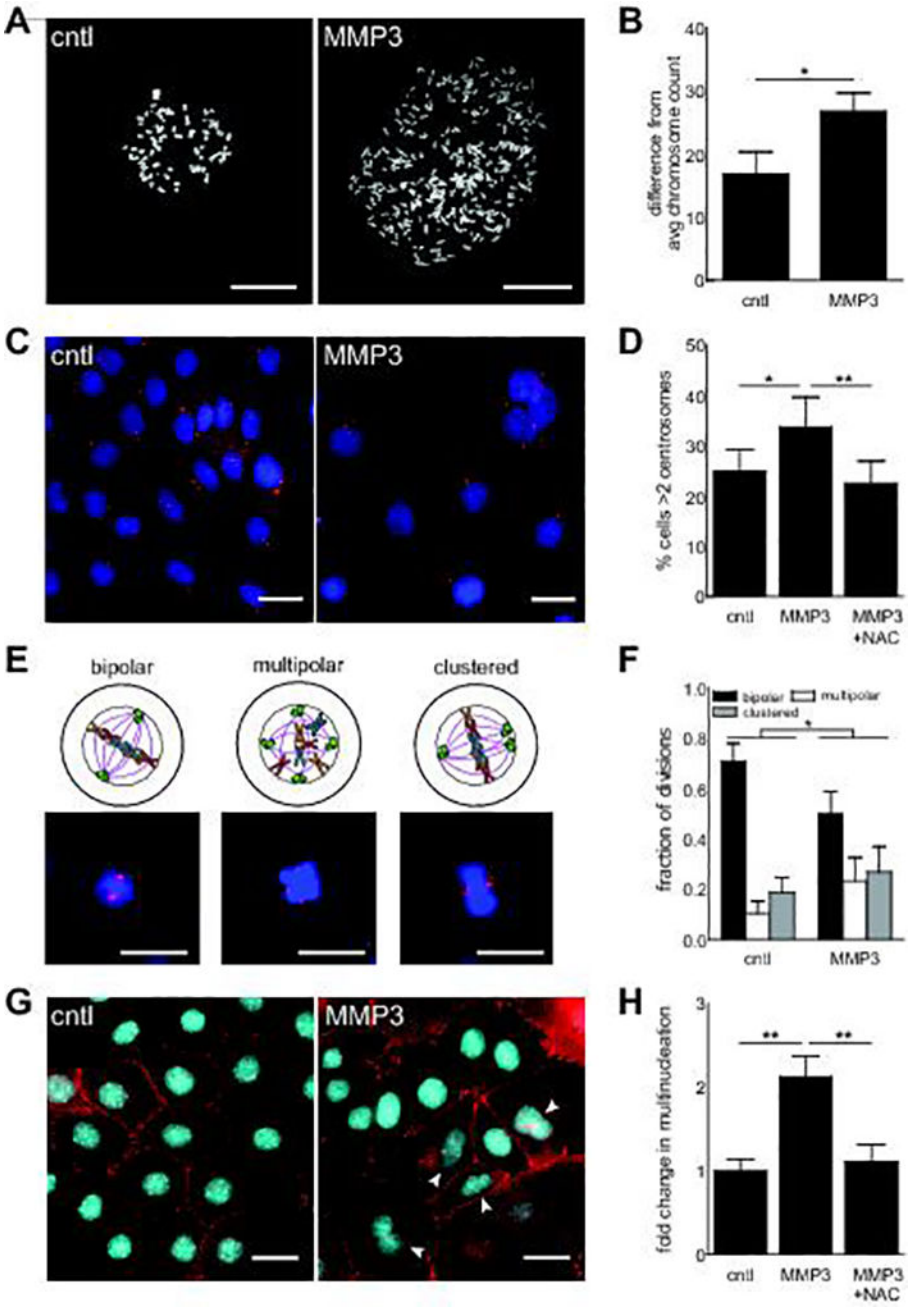

Figure 1. MMP3 induces chromosomal instability, centrosome amplification, mitotic abnormalities, and multinucleation

(**A,B**) Metaphase spreads of SCp2 mouse mammary epithelial cells treated with or without MMP3. (**C,D**) MMP3-induced ROS cause centrosome amplification. Red, γ-tubulin; blue, DNA. (**E,F**) Multipolar and clustered mitoses in cells treated with or without MMP3. Red, γ-tubulin; blue, DNA. (**G,H**) MMP3 induces multinucleation. Red, E-cadherin; cyan, DNA. Cells were exposed to MMP3 for 72 hr. Arrowheads denote multinucleated cells. Scale bars, 25 μm. Shown are mean ± S.E.M. for 3–7 experiments (n>30 cells for B; n>400 cells for D;

n>30 cells for F; n>150 cells for H). * $p < 0.05$, ** $p < 0.01$ (B, paired t-test; D, H, one-way ANOVA; F, two-way ANOVA).

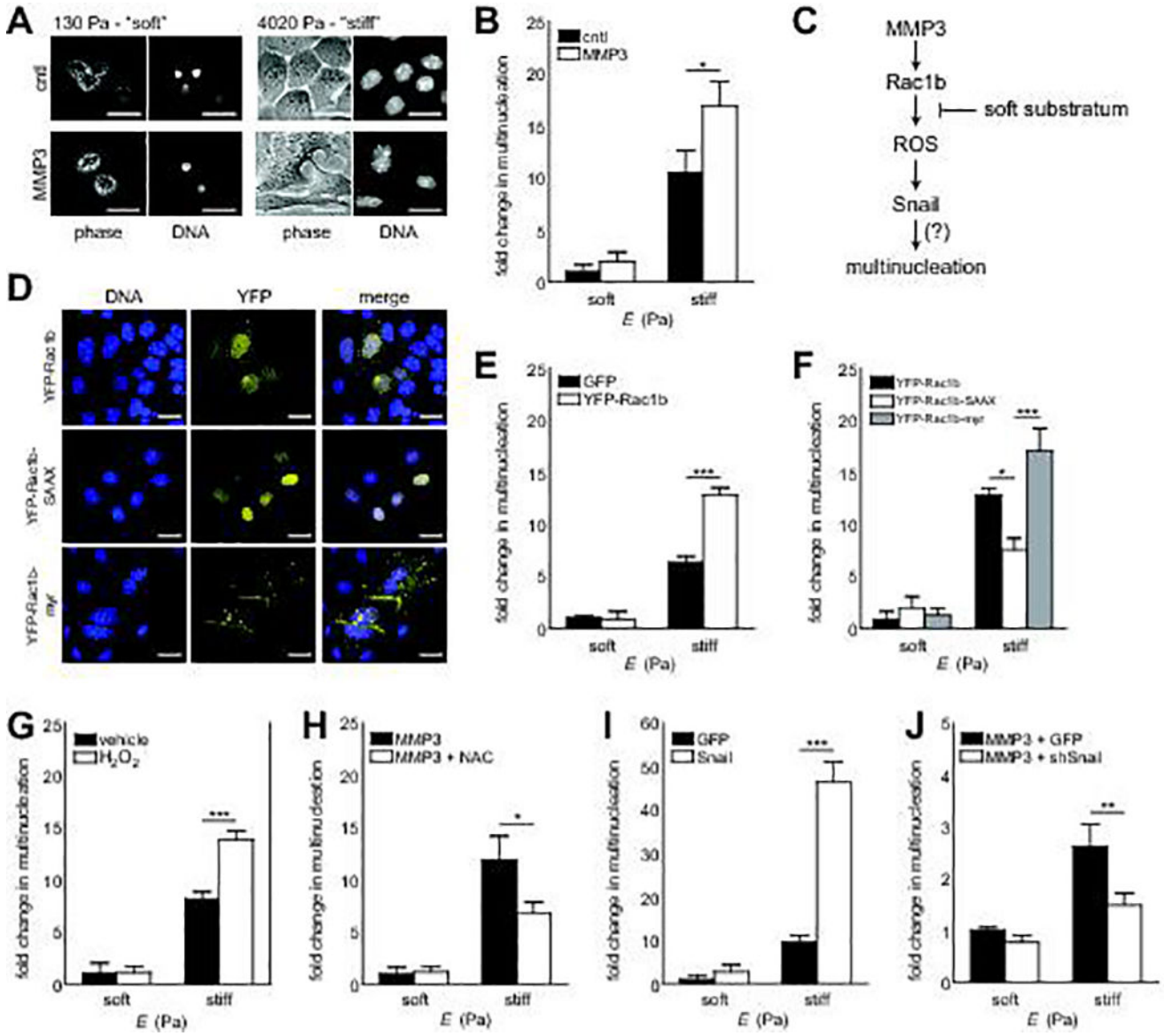

Figure 2. Substratum stiffness regulates multinucleation downstream of MMP3, Rac1b, ROS, and Snail

(**A**) SCp2 mouse mammary epithelial cells were cultured on soft or stiff substrata in the presence or absence of MMP3. (**B**) MMP3 induces multinucleation on stiff substrata only. (**C**) MMP3 induces the expression of Rac1b, causing an increase in production of ROS and elevated expression of Snail, resulting in multinucleation. (**D–F**) Multinucleation on stiff substrata depends on localization of Rac1b to the membrane. (**G–J**) ROS and Snail induce multinucleation on stiff substrata. Blocking these signals reduces multinucleation on stiff substrata. Culture on soft substrata prevents multinucleation. Cells were exposed to MMP3, ROS, or ROS+NAC for 72 hr (panels B, G, H), or expressed Snail or Rac1b variants for 48 hr (panels E, F, I, J). Scale bars, 25 μm. Shown are mean ± S.E.M. for 3–6 experiments (n>80 cells for B; n>100 cells for E; n>100 cells for F; n>100 cells for G; n>50 cells for H; n>80 cells for I; n>200 cells for J). * $p < 0.05$, *** $p < 0.001$ (two-way ANOVA).

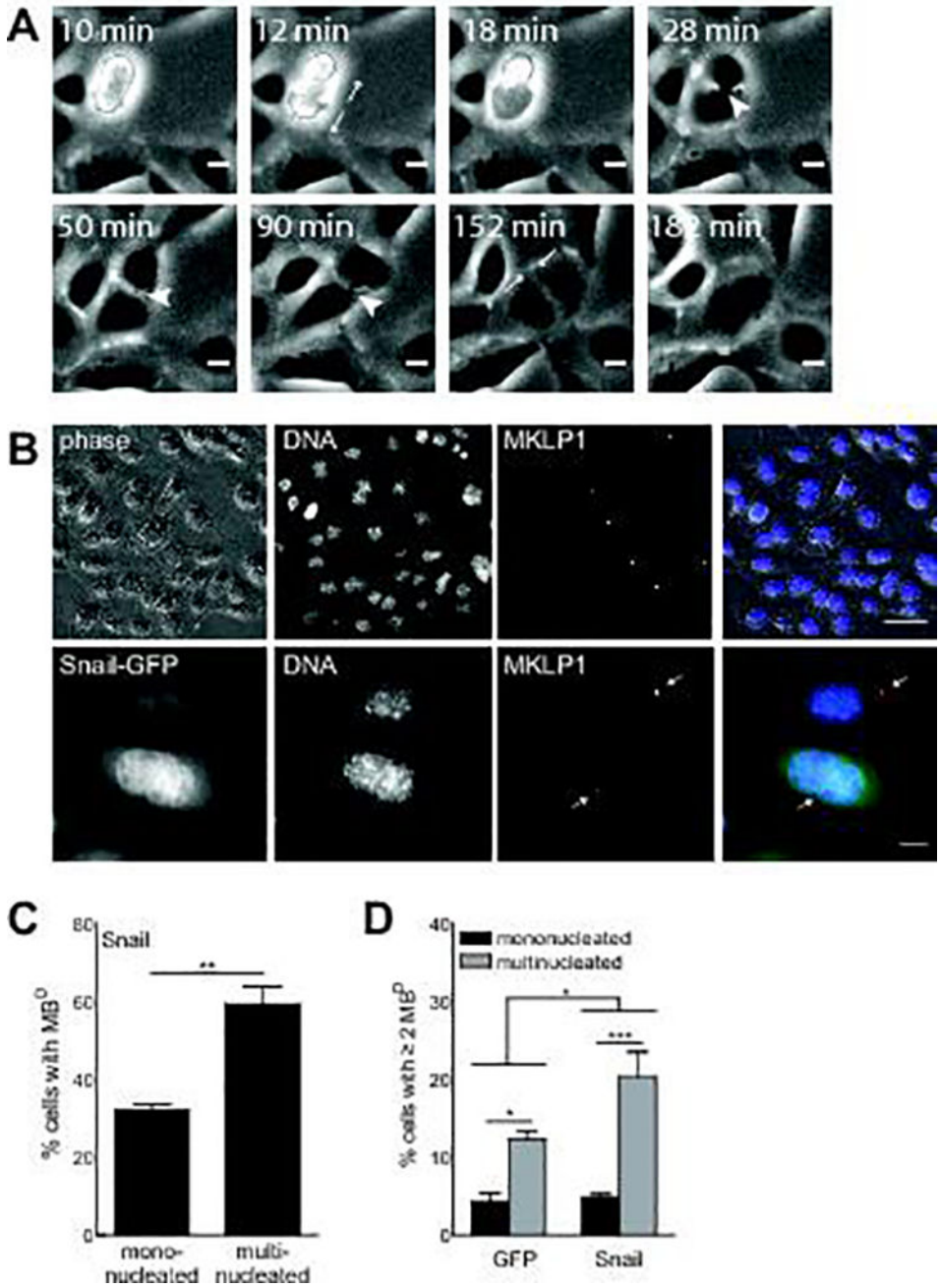

Figure 3. Snail-induced multinucleation follows midbody persistence

(**A**) Persistent midbodies (arrowheads) are visible between sister SCp2 mouse mammary epithelial cells that later merge to form a multinucleated cell. Images extracted from timelapse microscopy. Scale bars, 10 μm. See also Movie S1 and S2. (**B**) MB^Ds in cells ectopically expressing Snail are quantified by MKLP1-positive puncta. Red, MKLP1; green, Snail-GFP; blue, DNA. Top row scale bars, 50 μm. Bottom row scale bars, 10 μm. Arrows in bottom row indicate MB^Ds. (**C**) A higher fraction of multinucleated cells ectopically expressing Snail have MB^Ds than mononucleated cells expressing Snail. (**D**) Multinucleated cells accumulate more MB^Ds than do mononucleated cells. This difference is exacerbated in

cells expressing Snail as compared to those expressing GFP alone. Cells expressed GFP or Snail for 48 hr. Shown are mean ± S.E.M. for 3 experiments (n>500 cells for C, D). * $p < 0.05$, *** $p < 0.001$ (C, paired t-test; D, two-way ANOVA).

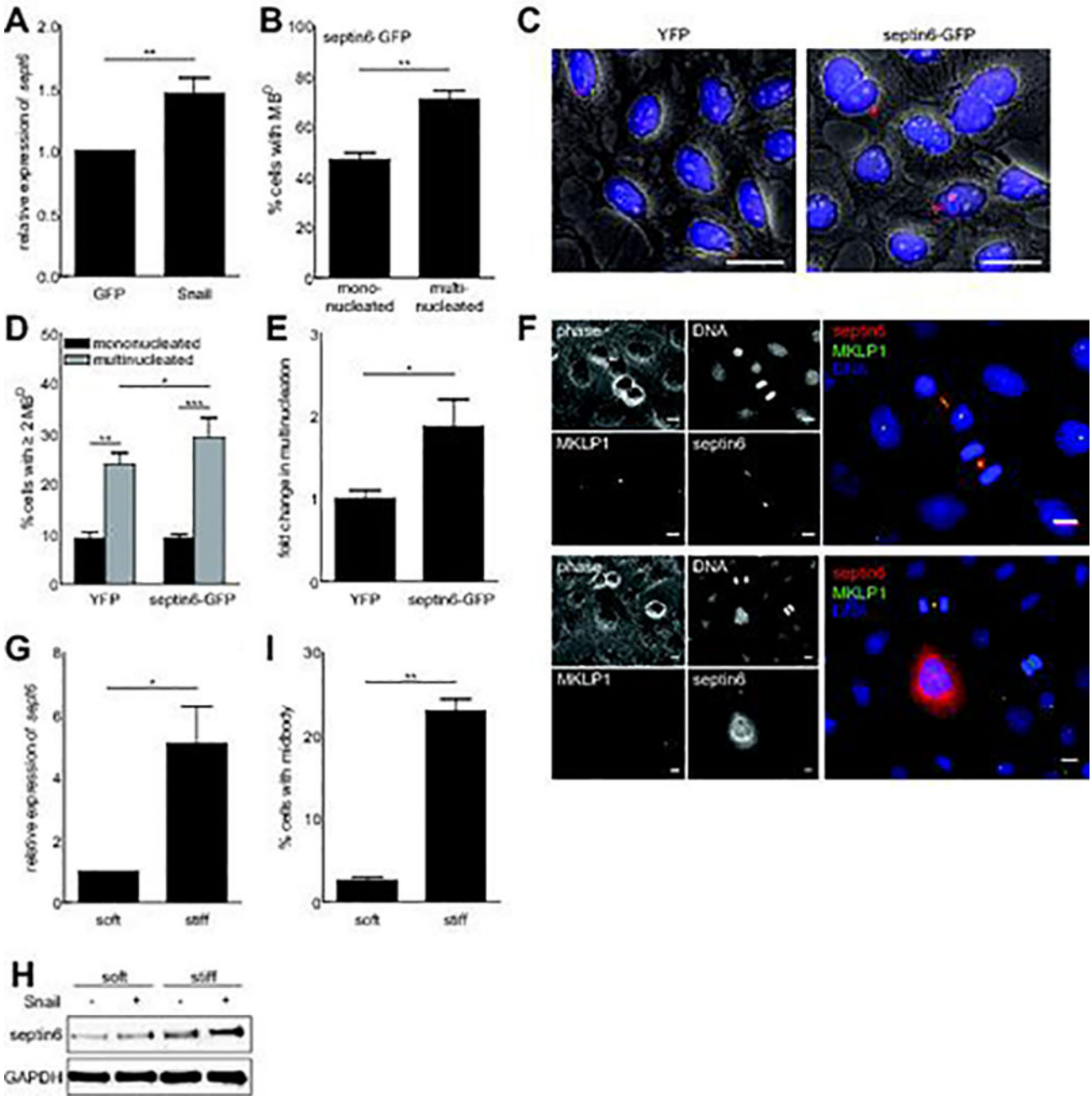

Figure 4. Snail and substratum stiffness induce midbody persistence via septin-6

(**A**) Ectopic expression of Snail causes an increase in the levels of septin-6 in SCp2 mouse mammary epithelial cells. Expressing a septin6-GFP fusion protein induces (**B**) midbody persistence, (**C,D**) midbody accumulation, and (**E**) multinucleation. Red, MKLP1; blue, DNA. Scale bars, 50 μm. (**F**) SCp2 mouse mammary epithelial cells expressing septin6-GFP show that septin-6 colocalizes with the midbody marker MKLP1. Red: septin6-GFP; green: MKLP1; blue: DNA. Scale bars, 10 μm. (**G**) Cells cultured on stiff substrata express a higher level of septin-6 than cells on soft substrata. (**H**) Ectopic expression of Snail (+) in SCp2 mouse mammary epithelial cells induces the expression of septin-6 protein on stiff but not

soft substrata. Control cells (−) were transduced with GFP alone. (**I**) A higher fraction of cells cultured on stiff substrata have MB^Ds than cells on soft substrata. Cells were transfected with plasmid 48 hr before analysis. Shown are mean ± S.E.M. for 3–10 experiments (n>800 cells for B,D; n>800 cells for E; n>200 cells for I). * $p < 0.05$, ** $p < 0.01$, *** $p < 0.001$ (A, B, E, G, I, paired t-test; D, two-way ANOVA).

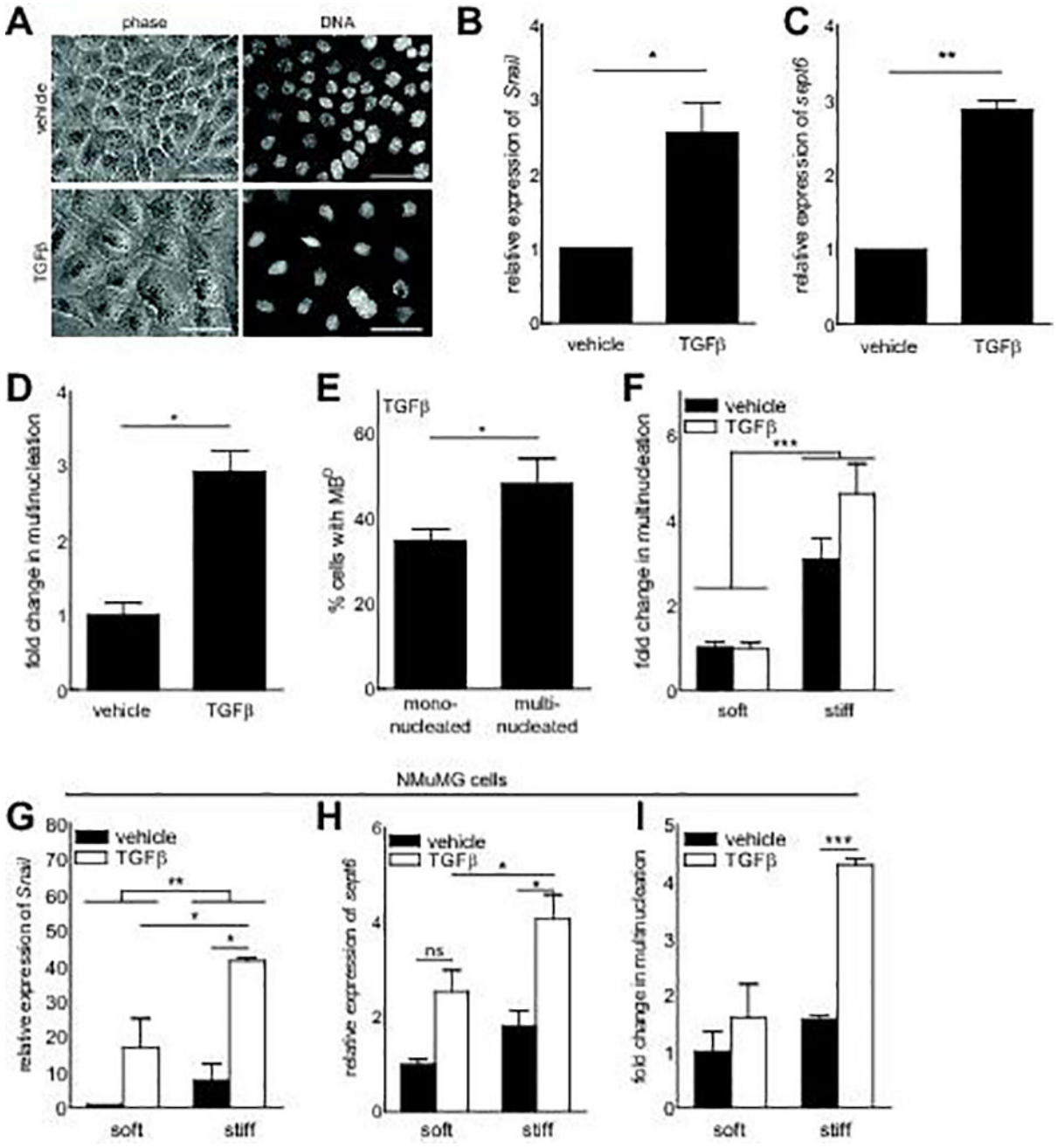

Figure 5. TGFβ induces Snail, increases septin-6, and leads to multinucleation

(**A**) SCp2 mouse mammary epithelial cells were cultured on soft or stiff substrata in the presence or absence of TGFβ. Treatment with TGFβ increases the levels of (**B**) Snail and (**C**) septin-6, and (**D**) induces multinucleation. (**E**) A higher fraction of multinucleated cells had MB^Ds than did mononucleated cells. (**F**) TGFβ-induced multinucleation is blocked in cells cultured on soft substrata. Treatment with TGFβ increases the expression of (**G**) Snail, (**H**) septin-6, and (**I**) multinucleation in NMuMG mouse mammary epithelial cells cultured on stiff substrata. Cells were exposed to TGFβ for 48 hr. Scale bars, 50 μm. Shown are mean

± S.E.M. for 3–6 experiments (n>500 cells for D; n>30 cells for E; n>170 cells for F). * $p < 0.05$, ** $p < 0.01$, *** $p < 0.001$ (B–E, paired t-test; F–H, two-way ANOVA).

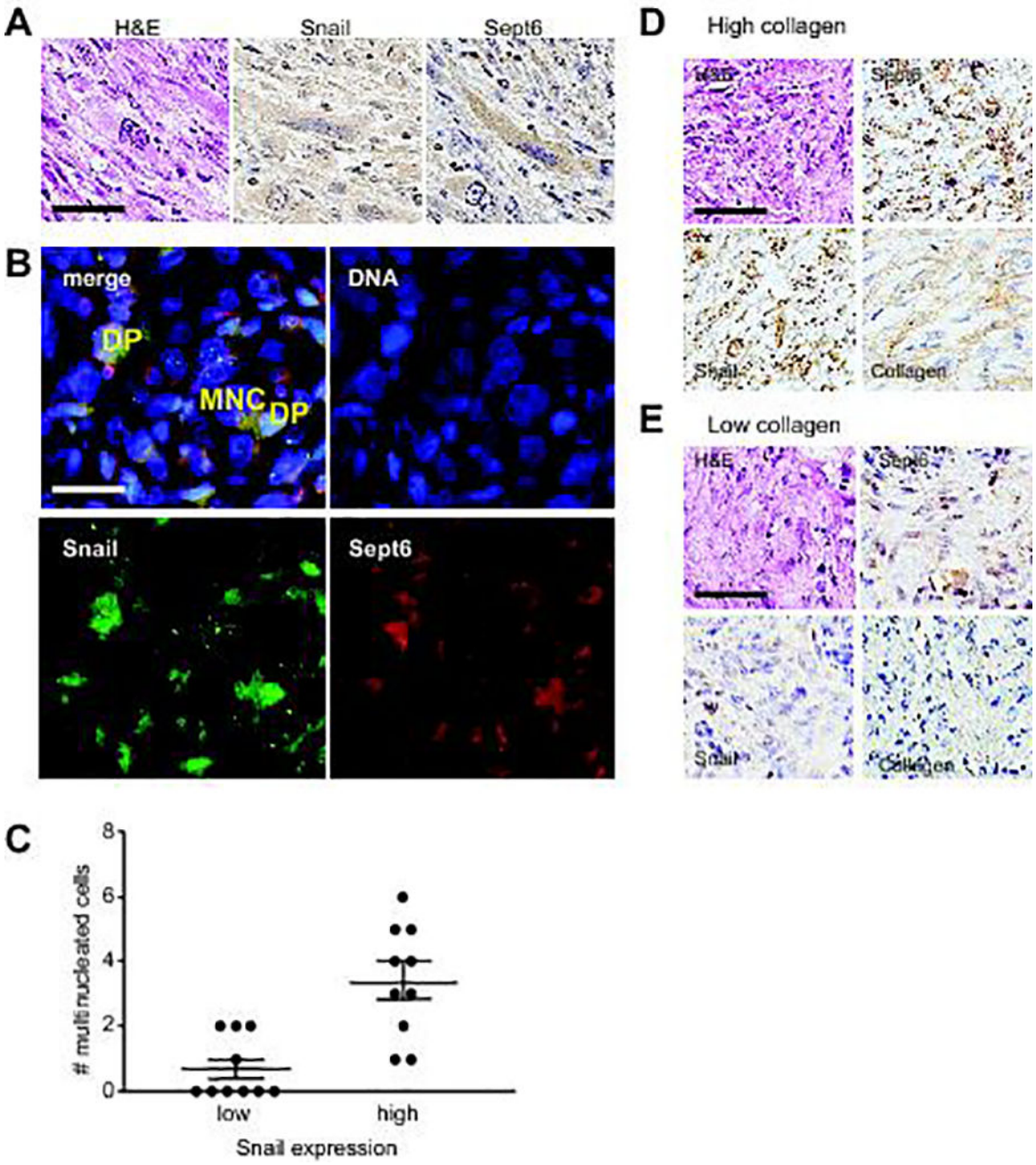

Figure 6. Multinucleation is elevated in regions of high Snail expression in metaplastic carcinoma

(**A**) Immunohistochemistry analysis for Snail and septin-6 in human breast metaplastic carcinoma. Scale bar, 100 μm. (**B**) Immunofluorescence analysis of human breast metaplastic carcinoma reveals multinucleation (MNC) in cells double-positive (DP) for Snail and septin-6. Scale bar, 50 μm. (**C**) Quantification of multinucleated cells in regions of high and low Snail expression. p = 0.007 (Mann-Whitney test). Immunohistochemistry analysis of human breast metaplastic carcinoma reveals elevated expression of Snail and septin-6 in regions of (**D**) high collagen compared to (**E**) low collagen. Scale bars, 100 μm.

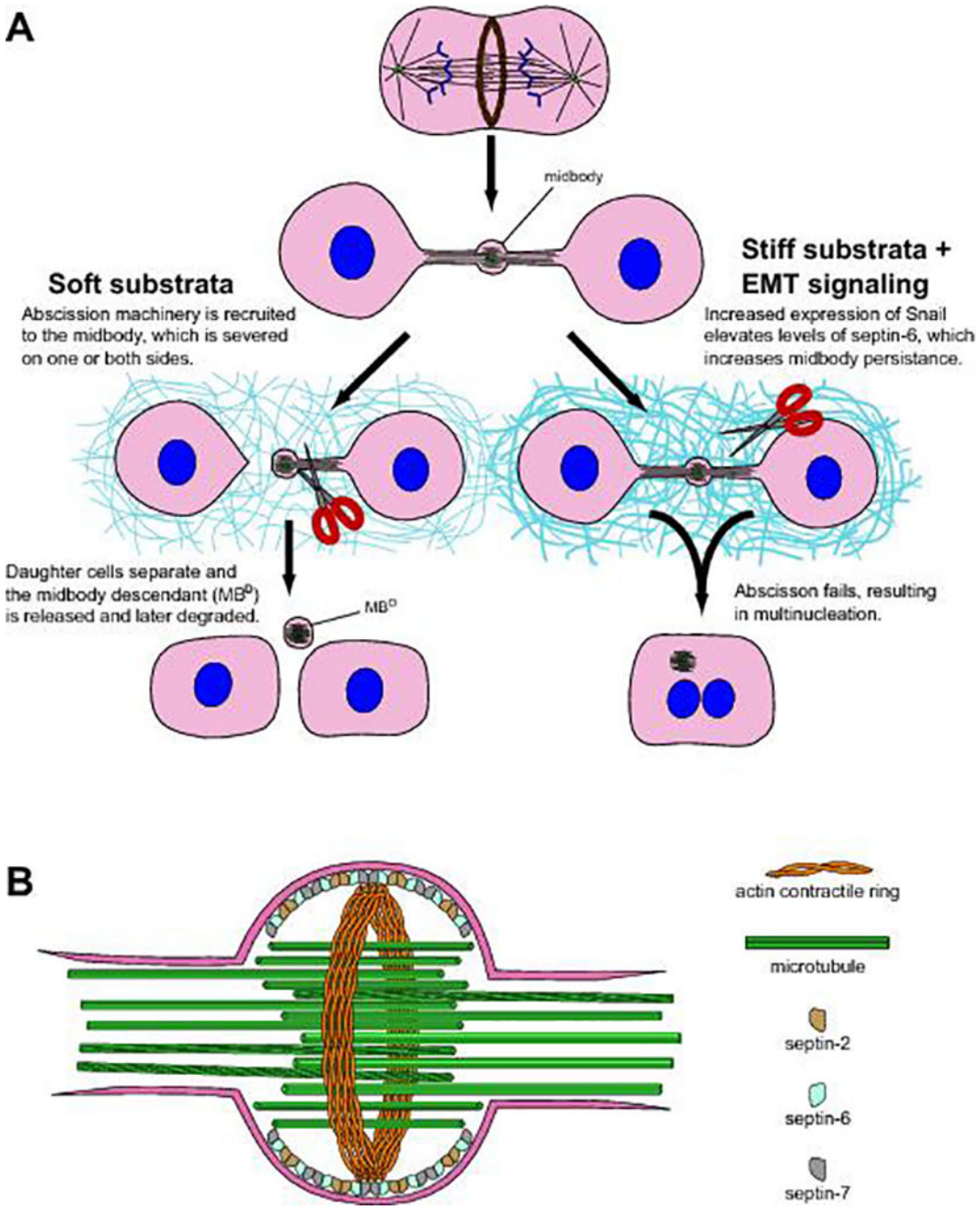

Figure 7. Stiffness modulates multinucleation downstream of EMT signaling

(**A**) EMT inducers MMP3 and TGFβ lead to increased expression of Snail, which increases midbody persistence, abscission failure, and multinucleation on stiff microenvironments only. (**B**) Elevated levels of septin-6 downstream of Snail may disrupt the function of septin filaments, which help anchor the contractile ring to the plasma membrane.